

Original Article

Long non-coding RNA HOXA11-AS protects the barrier function of corneal endothelial cells by sponging microRNA-155 to alleviate corneal endothelial injury

Shuyi Yuan^{1,2}, Xiaoyong Yuan^{1,2}, Lihua Li^{1,2}

¹Clinical College of Ophthalmology, Tianjin Medical University, Tianjin 300070, China; ²Tianjin Key Laboratory of Ophthalmology and Visual Science, Tianjin Eye Institute, Tianjin Eye Hospital, No. 4 Gansu Road, He-ping District, Tianjin 300000, China

Received May 24, 2022; Accepted August 31, 2022; Epub December 15, 2022; Published December 30, 2022

Abstract: Objectives: Corneal endothelial cells (CECs) are extremely vulnerable to injury. In this study, the role and mechanism of action of the long non-coding RNA HOXA11-AS during corneal endothelial injury (CEI) were evaluated in vivo and in vitro. Methods: Scratch wounds were made to induce CEI in the corneal endothelium of rats and mice. Homeobox A11 (HOXA11)-AS expression was determined at different time points using quantitative real-time PCR. Human CECs with HOXA11-AS overexpression or downregulation were examined for survival, ferroptosis, and migration. Bioinformatics and dual-luciferase reporter assays were used to investigate the correlation between HOXA11-AS and microRNA (miR)-155. Results: HOXA11-AS expression was reduced in the corneal endothelium in a time-dependent manner. Scratch wounds triggered high rates of ferroptosis and migration in CECs and impaired cell proliferation. HOXA11-AS overexpression partially attenuated the scratch wound-induced changes in proliferation, ferroptosis, and migration, whereas silencing HOXA11-AS had the opposite effects. Moreover, HOXA11-AS served as a competing endogenous RNA of miR-155. Levels of miR-155 were upregulated in the corneal endothelium following the scratch injury, and this upregulation abolished the effect of HOXA11-AS overexpression on the behavior of CECs after injury; miR-155 inhibition counteracted the effect of HOXA11-AS silencing. Conclusions: HOXA11-AS exerts protective effects against CEI by sponging miR-155, suggesting that these loci are treatment targets for corneal endothelial disorders.

Keywords: Corneal endothelial injury, corneal endothelial cell, HOXA11-AS, microRNA-155, ferroptosis, migration

Introduction

The corneal endothelium is a monolayer formed by hexagonal cells that present a leaky obstacle between the aqueous humor in the anterior chamber of the eye and the corneal stroma. The major role of the corneal endothelium is to provide a slightly dehydrated condition (known as corneal deturgescence) for the corneal stroma, which is needed for optical transparency. The leaky obstacle is due, at least in part, to the discontinuous tight junction protein zonula occludens-1 (ZO-1) [1]. To balance liquid flow into the stroma, endothelial cells are capable of actively transporting fluid back to the anterior chamber by ion transporters, such as Na⁺K⁺-ATPase pumps [2]. Disorders that can influence the “pump-leak” balance will cause a loss of

corneal transparency and stromal edema, leading to irreversible vision loss [3]. Corneal transplantation is the only efficient way to restore vision in patients with endotheliopathy. The need for donor corneas has prompted investigators to explore the feasibility of using expanded corneal endothelial cells (CECs) as a treatment option by anterior chamber cell injection or tissue engineering [4].

CECs exist in the innermost corneal layer and are important for corneal transparency, since they act as a barrier and as “ion pumps” [5]. Cell cycle arrest of human CECs (hCECs) occurs at the G1 phase; therefore, the division of human CECs does not occur in vivo [6]. In normal conditions, a mean loss rate of 0.3-0.6% CECs can be detected each year; however, adja-

cent cells can surround the wound area by migration and/or spreading. Thus, CECs are capable of maintaining a fluid inlet/outlet balance and corneal transparency in a compensatory manner [7]. However, corneal surgeries, extra traumas, and stresses from glaucoma or endothelial dystrophies have the potential to dramatically decrease the cell density, eventually causing residual CEC decompensation [8]. When the human CEC density is reduced to <500-1000 cells/mm², redundant aqueous humor storage in the corneal stroma may result in bullous keratopathy, corneal edema, and visual acuity loss [9]. Some studies have indicated that topical Rho kinase (ROCK) inhibitors are capable of facilitating the recovery of the cryoinjured corneal endothelium [10, 11]. Y-27632, a ROCK inhibitor, has been experimentally used in patients with bullous keratopathy during cultivated human CEC transplantation [12]. Owing to the risk of endothelial-mesenchymal transition (EMT) and limitations in the ex vivo expansion of human CECs, medicinal or new grafting treatments suitable for patients suffering from corneal endothelial decompensation are lacking [13, 14]. Thus, it is necessary to investigate novel therapeutic methods, intrinsic biological and molecular mechanisms, and essential factors involved in corneal endothelial injury (CEI).

Long non-coding RNAs (lncRNAs) are critical in many diseases, especially tumors, as they participate in various biologic processes, such as mRNA selective splicing, epigenetic and post-translational modulation, chromatin modification, and microRNA (miRNA) decoy activity [15-17]. Many studies have indicated that cytoplasmic lncRNAs function as sponges capable of sequestering miRNAs to control the expression of other RNAs [18, 19]. Homeobox A11 (HOXA11)-AS has recently been identified as a critical tumor-promoting lncRNA in many cancers, such as squamous cell cancer [20], gastric cancer [21], breast cancer [21], and non-small-cell lung carcinoma [22]. However, the role of HOXA11-AS in CEI has not been established.

In the present study, scratch wounds were made to induce CEI in the corneal endothelium of rats and mice. HOXA11-AS expression was evaluated under both normal and injured conditions. Loss- and gain-of-function studies were performed to assess the role of HOXA11-

AS in CEI damage and the underlying molecular mechanisms. Our findings indicate that HOXA11-AS exerts protective effects against CEI.

Material and methods

CEI model establishment

Male BALB/c mice (aged 56 days) and male SD rats (aged 42 days) were provided by the Tianjin Experimental Animal Center. All experiments were approved by the Animal Care and Experiment Committee of Tianjin Medical University. All operations were conducted in accordance with the Association for Research in Vision and Ophthalmology (ARVO) Statement for animal use. Rats and mice were kept in different colony rooms with a 12-h light/dark cycle at 25°C for 7 days prior to the experiments. All animals were arbitrarily classified into injured and control groups. A scratch wound model of the corneal endothelium was constructed. In brief, animals were anesthetized by an intra-abdominal injection of pentobarbital sodium and topical oxybuprocaine. Under a stereoscopic microscope, a 30-gauge needle was inserted into the anterior chamber of the eye through the limbus, and an endothelial wound was made by gently scraping cells, taking care not to collapse the anterior chamber or to damage Descemet's membrane. Researchers were blinded to the group assignment in the process of data collection and analysis [23].

Hematoxylin and eosin (H&E) staining

After fixation for 16-18 h with paraformaldehyde (4%), the corneal samples were exposed to ethanol (EtOH) dehydration at various concentrations (70%, 80%, 90%, 95%, and 100%), rinsed twice with xylene (X820585, 500 mL) for 300 s each time, embedded in paraffin, and sectioned (thickness, 4 µm). The paraffin-embedded sections were dewaxed with water, subjected to hematoxylin staining (C0007) for 10 min at room temperature (RT), rinsed with running water for 0.5-1 min, differentiated with 1% hydrochloric acid alcohol for 60 s, and rinsed with running water for 60 s. The sections were then stained with eosin for 5-10 min at RT, dehydrated in the EtOH gradient mentioned above for 60 s, rinsed twice with xylene for 60 s each time, and mounted in neutral balsam. Pathologic changes were observed using a fluorescence microscope (Zeiss, Oberkochen, Germany).

HOXA11-AS in corneal endothelial injury

Table 1. Sequences of primers in qRT-PCR

Primer	Sequence
HOXA11-AS F	5'-TCT CCT GGA GTC TCG CAT TT-3'
HOXA11-AS R	5'-TCG GAA GTG ACC ATG AAT GA-3'
miR-155 F	5'-TAA AAA GGA CAG GAA TAC A-3'
miR-155 R	5'-CAAGTCTTCAGATACAATG-3'
GAPDH F	5'-GGG CAT GAA CCA TGA GAA GT-3'
GAPDH R	5'-AAG CAG GGA TGA TGT TCT GG-3'
U6 F	5'-GCT TCG GCA GCA CAT ATA CTA AAA T-3'
U6 R	5'-CGC TTC ACG AAT TTG CGT GTC AT-3'

CEC scratch assay

B4G12 cells (an authenticated human immortalized CEC line) were obtained from Creative Bioarray Company and cultivated in Dulbecco's modified Eagle's medium supplemented with 10% fetal bovine serum. Wounds were inflicted by scratching with a sterile pipette tip and harvested for subsequent analyses 0.5 days after wounding.

Transfection

To generate CECs with high or low HOXA11-AS levels, pcDNA3.1-HOXA11-AS or HOXA11-AS siRNA was first synthesized (GenScript) and confirmed by sequencing (Ruibiotech). CECs were transfected with pcDNA3.1-HOXA11-AS, pcDNA3.1-empty, HOXA11-AS siRNA (5'-CAG UUA UCA CAG UGC UGA UGC U-3'), or NC siRNA (5'-UUC UCC GAA CGU GUC ACG UTT-3') by Lipofectamine 2000 (Invitrogen, Waltham, MA, USA) to construct the lentivirus. The transfection efficiency was confirmed by qPCR.

All miR-155 mimic (5'-UUA AUG CUA AUC GUG AUA GGG GU-3'), inhibitor (5'-UUA AUG CUA AUC GUG AUA GGG GU-3'), NC mimic (5'-UUG UAC UAC ACA AAA GUA CUG-3'), and NC inhibitor (5'-UCA CAA CCU CCU AGA AAG AGU AGA-3') were purchased from RiboBio (Guangzhou, China) and diluted to 50 nM. CECs were transfected with the miR-155 inhibitor, mimic, or NC using Lipofectamine 2000 (Invitrogen), according to the manufacturer's instructions. The transfection efficiency was confirmed by qPCR.

Reverse transcription and quantitative real-time PCR (qRT-PCR)

Total RNA was isolated with TRIzol (Invitrogen) according to the manufacturer's protocol and subjected to RNase-free DNase 1 incubation to

remove contaminating DNA. PCR (30 cycles) was used to amplify the glyceraldehyde 3-phosphate dehydrogenase (*GAPDH*) and *U6* small nuclear RNA genes to validate the genomic DNA and RNA deletion. RNA (2 μ g) was then reverse-transcribed to obtain cDNA in a reaction mixture (20 μ L) containing dNTPs (2 μ M), random hexamers (2.5 μ M), and M-MLV reverse transcriptase (200 U). qRT-PCR was then conducted using an ABI PRISM 7300 Real-time Cyclor as follows: initial denaturation, 3 min at 95°C; 40 cycles of 10 s at 95°C, 30 s at 58°C, and 30 s at 72°C. Relative mRNA expression of the target gene was measured using the $2^{-\Delta\Delta CT}$ method, as described in the User Bulletin of Applied Biosystems No. 2 (P/N 4303859) [24], using *GAPDH* and *U6* as internal references. The primers used in this experiment are displayed in **Table 1**.

Western blotting (WB)

B4G12 cell lysis was performed in RIPA buffer for 0.5 h on ice. Cell lysates were then centrifuged for 20 min at 12,000 \times g, and the protein concentration was determined using a BCA Kit (Dingguo Company; catalog no: P0012). Cell lysates (30 mg) were subjected to sodium dodecyl sulfate-polyacrylamide gel electrophoresis (SDS-PAGE) for western blotting (WB). The antibodies used for WB were as follows: anti-GPX antibody (1:2500, ab153969; Abcam, Cambridge, UK), anti-SLC7A11 antibody (1:1000, ab37185; Abcam), anti-ACSL4 antibody (1:5000, ab155282; Abcam), anti-ZO-1 antibody (1:2500, ab216880; Abcam), anti-N-cadherin antibody (1:2500, ab76057; Abcam), anti-E2F2 antibody (1:2500, ab235837; Abcam), and anti-Tubulin antibody (1:5000, ab7291; Abcam). The blots were rinsed with Tris-buffered saline plus Tween 20 (TBST) extensively and examined by chemiluminescence (Chemi-Doc XRS; Bio-Rad, Hercules, CA, USA).

Cell Counting Kit (CCK)-8 assay

Cell viability was evaluated by the CCK-8 assay. In brief, plated B4G12 cells were exposed to CCK-8 (0.5 mg/mL, 10 μ L) and incubated for 60 min. The absorbance of cells at 450 nm was determined using an Infinite M200 microplate reader (Tecan, Männedorf, Switzerland) to evaluate cell viability.

HOXA11-AS in corneal endothelial injury

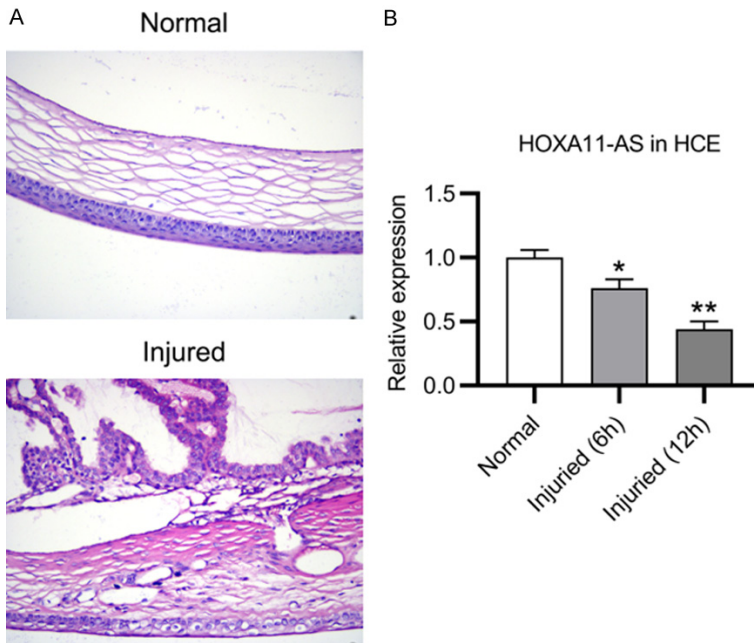


Figure 1. Homeobox A11 (HOXA11)-AS expression in the injured corneal endothelial tissue. The right eye of mice ($n = 8$ in each group) was subjected to corneal endothelial scratch to establish an injury model. A. Hematoxylin and eosin (H&E) staining was performed to examine the pathogenic alterations of the corneal endothelium. B. HOXA11-AS expression in the corneal endothelium was determined via qRT-PCR at 6 h and 12 h post-modeling. * $P < 0.05$, ** $P < 0.01$ vs. Normal group.

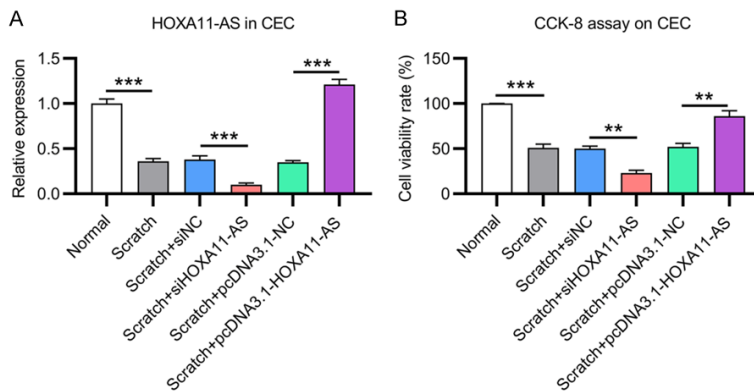


Figure 2. Expression of HOXA11-AS in the scratch-injured B4G12 cells. Wounds on B4G12 cells were made by scratching via a sterile pipette tip. B4G12 cells were transfected with siRNA-HOXA11-AS or pcDNA3.1-HOXA11-AS or corresponding negative controls (NC) and were collected at 12 h after scratching for further analyses. A. HOXA11-AS expression in B4G12 cells was determined by qRT-PCR. B. B4G12 cell viability was examined by the CCK-8 assay. ** $P < 0.01$, *** $P < 0.001$.

Intracellular and lipid reactive oxygen species (ROS) measurements

B4G12 cells were first inoculated into six-well plates (3×10^5 cells/well). One day later,

the cells were subjected to a scratch assay for 0.5 days. 2'-7'-Dichlorofluorescein diacetate (DCFH-DA) or the C11 BODIPY fluorescent probe was used to determine intracellular ROS or lipid ROS levels, respectively. Briefly, cells were rinsed three times with PBS and exposed to DCFH-DA ($10 \mu\text{M}$) or C11 BODIPY ($5 \mu\text{M}$) at 37°C for 20 min in the dark. After incubation, fluorescence intensity (Excitation 488 nm , Emission 525 nm) was determined using a SpectraMax® M5 fluorescence microplate reader.

Apoptosis determination

The quantification of dead cells was performed by flow cytometry (FC) using Annexin V-Fluorescein Isothiocyanate/Propidium Iodide (Annexin V-FITC/PI) Apoptosis Detection Kits (BD Pharmingen, San Diego, CA, USA). Briefly, the cell suspension was incubated with Annexin V-FITC ($10 \mu\text{L}$) and PI ($5 \mu\text{L}$) after preparation with binding buffer ($20 \mu\text{L}$). Apoptotic cells were assessed and identified by FC using FACS Diva (BD Biosciences, San Jose, CA, USA).

Cell migration determination assay

Confluent B4G12 cells were scratched with a pipette tip, allowed to move to the wound, and fixed. The scratched area was examined using a microscope. The migration proportion (%) was obtained as $\text{width}_{2d} / \text{width}_{0d}$.

Statistical analyses

The results are displayed as mean \pm standard deviation (SD). Comparison among multiple groups was conducted using analysis of vari-

ance (ANOVA) followed by a Fisher's least significant difference (LSD) test for post-hoc analysis. Statistical significance was set at $P < 0.05$.

Results

CEI modeling induced the downregulation of HOXA11-AS in mice

The right eyes of mice were subjected to CEI modeling, and edema corneal turbidity was evaluated to verify successful model establishment. H&E staining showed that the corneas of healthy mice were transparent and smooth, with micro-neovascularization. Corneal edema was detected in eyes with deeply covered matrices, white turbidity on the surface, and substantial neovascularization, indicating that scratching conditions could lead to corneal impairment and supporting successful CEI model construction (**Figure 1A**). Neovascularization and corneal epithelial cell conditions were also observed by H&E staining. The corneal epithelia in the control group were tightly arranged, with an intact cell morphology, without vessels in the stromal layer, and with evenly distributed dead cells. In the injured groups, the corneal epithelia and number of cell layers were reduced and showed vacuolization, and the matrix layer exhibited a substantial neovascularization and severe edema (**Figure 1A**). HOXA11-AS mRNA expression, examined by qRT-PCR, was downregulated in the injured corneal endothelium of rats in a time-dependent manner (**Figure 1B**). These results suggest that HOXA11-AS participated in the regulation of CEI.

HOXA11-AS expression and its role in the viability of scratch-treated B4G12 cells

We introduced a scratch injury in the B4G12 cell line to establish a cell-based CEI model for analyses of the role of HOXA11-AS in vitro. After the scratch wound was introduced, the HOXA11-AS mRNA expression level dramatically decreased in B4G12 cells relative to levels in the untreated control group (**Figure 2A**). Loss- and gain-of-function experiments were then initiated by silencing or overexpressing HOXA11-AS in B4G12 cells. After transfection for 48 h, qRT-PCR results confirmed that HOXA11-AS expression was significantly reduced or elevated, in injured B4G12 cells with silenced or over-

expressed HOXA11-AS, respectively (**Figure 2A**).

Scratch injury significantly reduced the survival of B4G12 cells, as assessed by a CCK-8 assay. HOXA11-AS downregulation further impaired cell viability in scratch-injured cells, whereas HOXA11-AS overexpression partially recovered the rate of cell survival in scratch-injured B4G12 cells (**Figure 2B**).

Ferroptosis induced by scratch injury is regulated by HOXA11-AS

FC was used to evaluate the influence of HOXA11-AS on apoptosis in injured B4G12 cells. First, HOXA11-AS overexpression attenuated the rate of apoptosis in B4G12 cells treated with scratch injury, whereas a HOXA11-AS deficiency further augmented apoptosis in injured cells (**Figure 3A**).

Intracellular and lipid ROS production are two important indicators of cellular oxidative stress. Both intracellular and lipid ROS levels were higher in scratch-injured B4G12 cells than in untreated cells. HOXA11-AS overexpression alleviated intracellular and lipid ROS levels, whereas HOXA11-AS silencing had the opposite effect (**Figure 3B, 3C**).

High rates of apoptosis and increased lipid ROS levels are two indicators of ferroptosis. Therefore, we examined the protein expression levels of ferroptosis markers GPX4, ACSL4, and SLC7A11 in scratch-injured B4G12 cells. Scratch injury suppressed glutathione peroxidase 4 (GPX4) and solute carrier family 7 member 11 (SLC7A11) expression but increased the expression of acyl-CoA synthetase long chain family member 4 (ACSL4) in B4G12 cells compared with levels in control cells. HOXA11-AS silencing further reduced GPX4 and SLC7A11 levels and promoted ACSL4 expression in injured cells, whereas its overexpression reversed these phenotypes in scratch-injured B4G12 cells (**Figure 3D**). These data indicated that scratch wound-induced ferroptosis in B4G12 cells was attenuated by HOXA11-AS.

HOXA11-AS promoted the migration of scratch-injured B4G12 cells

Next, we examined the role of HOXA11-AS in the migration of scratch-injured B4G12 cells.

HOXA11-AS in corneal endothelial injury

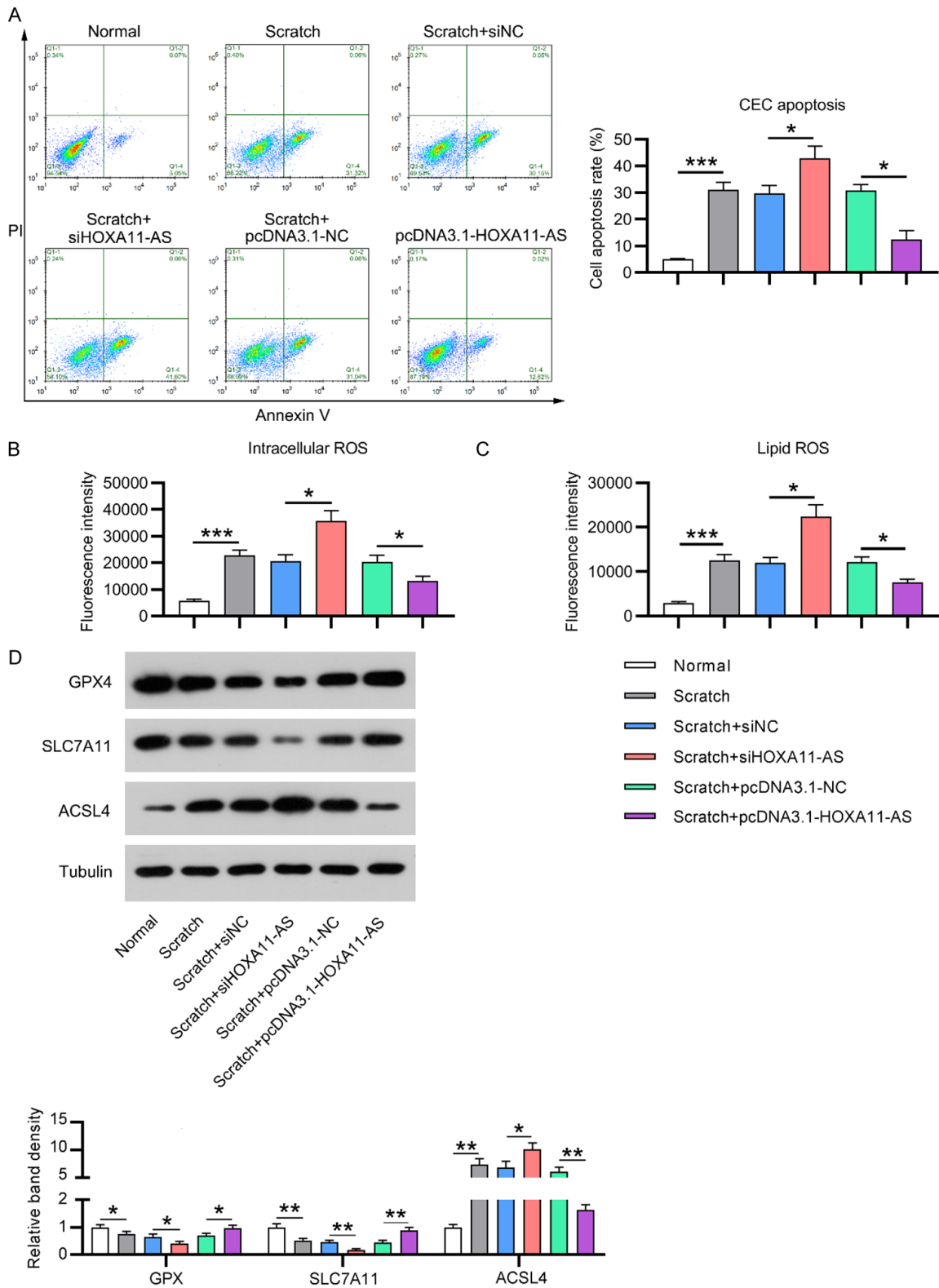


Figure 3. Effect of HOXA11-AS on scratch injury-induced ferroptosis in B4G12 cells. Wounds on B4G12 cells were made by scratching via a sterile pipette tip. B4G12 cells transfected with siRNA-HOXA11-AS or pcDNA3.1-HOXA11-AS or their negative controls (NC) were collected at 12 h after scratches for the subsequent analysis. (A) Apoptotic cells were counted by FC. The cell apoptosis rate in each group is shown on the right-hand panel. (B) DCFH-DA and (C) C11 BODIPY staining were performed to evaluate the production of intracellular and lipid reactive oxygen species (ROS) in B4G12 cells, respectively. (D) WB of glutathione peroxidase 4 (GPX4), acyl-CoA synthetase long chain family member 4 (ACSL4), and solute carrier family 7 member 11 (SLC7A11) expression in B4G12 cells. * $P < 0.05$, *** $P < 0.001$.

HOXA11-AS in corneal endothelial injury

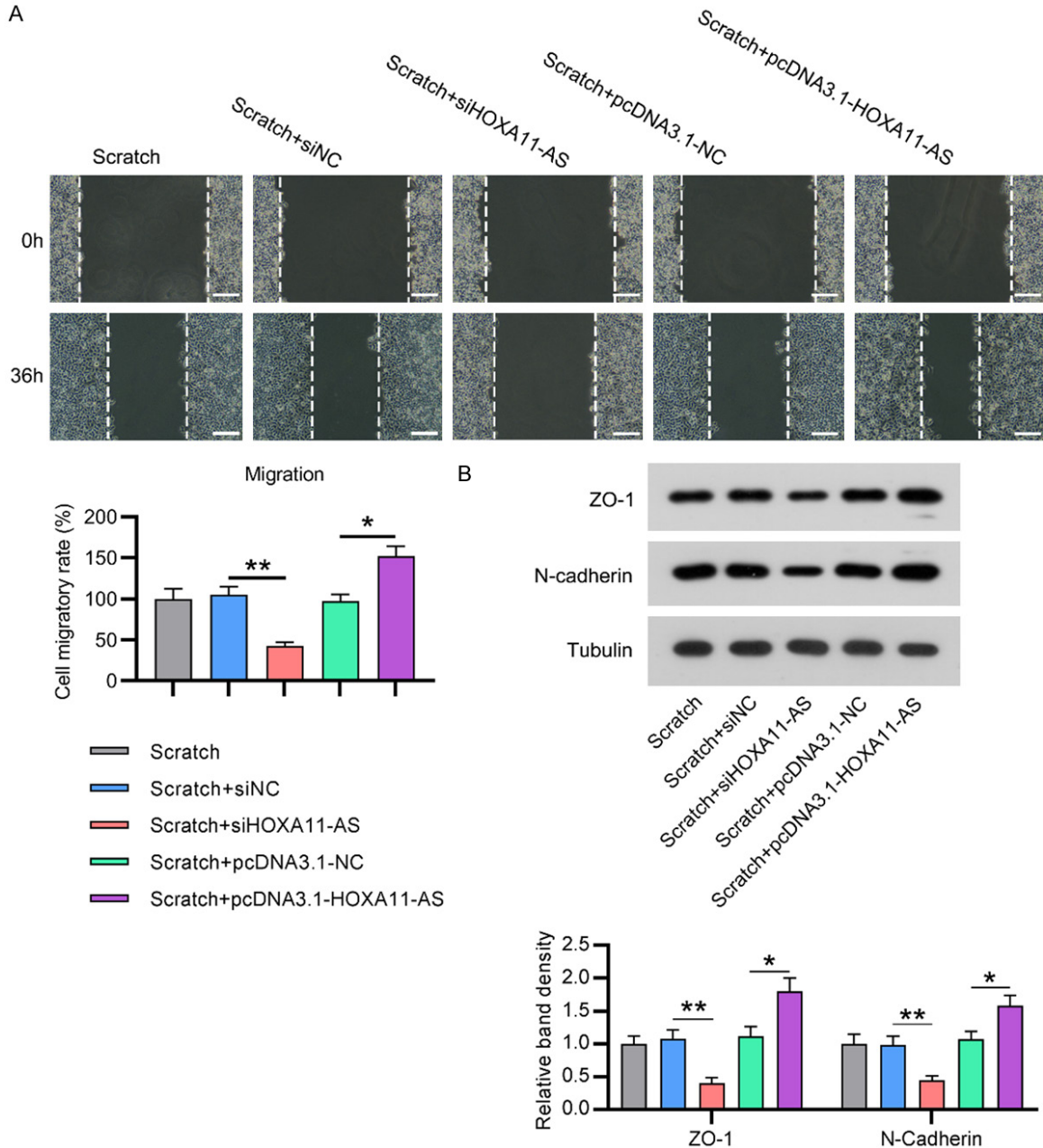


Figure 4. Role of HOXA11-AS in the migration of scratch-injured B4G12 cells. Wounds on B4G12 cells were made by scratching by a sterile pipette tip. B4G12 cells were transfected with siRNA-HOXA11-AS or pcDNA3.1-HOXA11-AS or their negative controls (NC) and were collected at 12 h after scratches for further analyses. A. The migration rate of B4G12 cells was determined by a scratch wound healing assay. B. Zonula occludens-1 (ZO-1) and N-cadherin protein expression levels were analyzed using WB. *P < 0.05, **P < 0.01.

The downregulation of HOXA11-AS in B4G12 cells led to a significant reduction in the rate of CEC migration, whereas HOXA11-AS overexpression increased the migratory capacity (Figure 4A). Furthermore, WB showed that the expression levels of tight junction proteins ZO-1 and N-cadherin were reduced by HOXA11-AS silencing and were upregulated after HOXA11-AS overexpression in B4G12 cells (Figure 4B).

These findings indicated that HOXA11-AS promoted the migration of scratch-injured B4G12 cells.

HOXA11-AS acts as a sponge RNA of miR-155-5p (miR-155)

A previous study demonstrated that the lncRNA HOXA11-AS and its target miR-155 mediate

HOXA11-AS in corneal endothelial injury

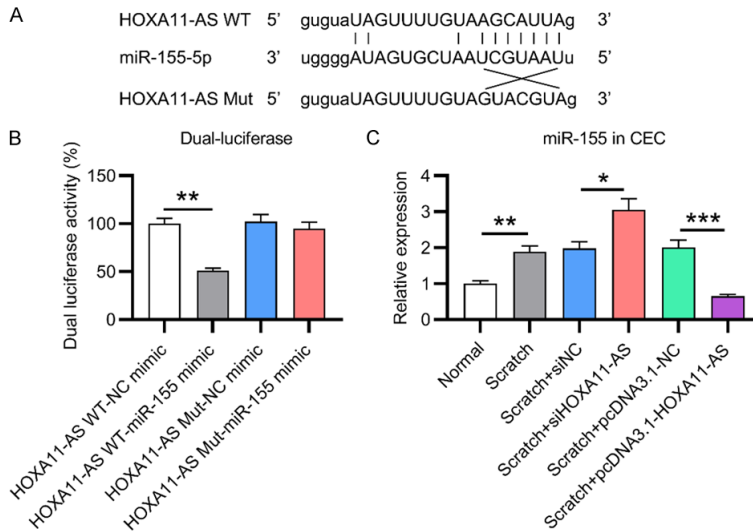


Figure 5. HOXA11-AS serves as a miR-155 ceRNA. **A.** Graphical representation of the conserved HOXA11-AS binding motif of miR-155. **B.** Dual-luciferase reporter assay (DLRA) using luciferase reporter constructs containing either mutant (Mut) or wild-type (WT) HOXA11-AS transfected with miR-155/NC mimic. Firefly luciferase activity was normalized against *Renilla* luciferase activity as a reference. **C.** Wounds on B4G12 cells were made by scratching via a sterile pipette tip. B4G12 cells transfected with siRNA-HOXA11-AS or pcDNA3.1-HOXA11-AS or their negative controls (NC) were collected at 12 h after scratches for further analyses. qRT-PCR was used to quantify miR-155 expression in B4G12 cells. * $P < 0.05$, ** $P < 0.01$, *** $P < 0.001$.

squamous cell carcinoma [20]. We, therefore, hypothesized that this axis might be involved in CEI and scratch-injured B4G12 cell phenotypes. A bioinformatic analysis clearly demonstrated that HOXA11-AS targeted miR-155 (Figure 5A). A dual-luciferase reporter assay of B4G12 cells confirmed that there was a negative correlation between HOXA11-AS and miR-155 (Figure 5B). Furthermore, scratch wounds resulted in the upregulation of miR-155 expression in B4G12 cells, which would be further augmented by HOXA11-AS silencing or ameliorated by HOXA11-AS overexpression (Figure 5C). These data suggested that HOXA11-AS acted as a ceRNA of miR-155 in CEI.

Involvement of miR-155 in the effects of HOXA11-AS on scratch-injured B4G12 cells

To evaluate the contribution of miR-155 to the HOXA11-AS-mediated viability of scratch-injured B4G12 cells, injured cells with silenced or overexpressed HOXA11-AS were transfected with a miR-155 inhibitor or mimic. qRT-PCR results showed that after transfection, miR-155 levels were reduced in B4G12 cells with silenced HOXA11-AS expression but elevated

in cells with overexpressed HOXA11-AS (Figure 6A, 6B).

A CCK-8 assay showed that the survival of scratch-injured B4G12 cells with silenced HOXA11-AS was restored by miR-155 inhibition (Figure 6C), whereas transfection with the miR-155 mimic decreased the viability of B4G12 cells with overexpressed HOXA11-AS (Figure 6D). These data suggested that miR-155 and HOXA11-AS exerted opposite effects in scratch-injured B4G12 cells.

miR-155 counteracted the effect of HOXA11-AS on scratch-injured B4G12 cell ferroptosis

We hypothesized that miR-155 counteracts the positive effect of HOXA11-AS on ferroptosis. To evaluate this hypothesis, we performed FC,

intracellular and lipid ROS detection, and ferroptosis marker expression analyses in scratched-injured B4G12 cells. miR-155 inhibition alleviated ferroptosis, decreased intracellular and lipid ROS levels, upregulated GPX4 and SLC7A11 expression levels, and downregulated ACSL4 levels in HOXA11-AS-silenced and scratch-injured B4G12 cells (Figure 7A-D). In contrast, the rate of apoptosis was significantly higher in HOXA11-AS-overexpressing and scratch-injured B4G12 cells with miR-155 upregulation. miR-155 upregulation also led to higher levels of intracellular ROS, lipid ROS, and ACSL4 expression, as well as decreased GPX4 and SLC7A11 protein levels (Figure 7E-H). These data clearly indicated that miR-155 counteracted the inhibitory effect of HOXA11-AS on scratch-injured B4G12 cell ferroptosis.

miR-155 abolished the effect of HOXA11-AS on the migration of scratch-injured B4G12 cells

Next, we determined the involvement of miR-155 in the HOXA11-AS-induced migration of scratch-injured B4G12 cells. A scratch wound healing assay showed that miR-155 inhibition

HOXA11-AS in corneal endothelial injury

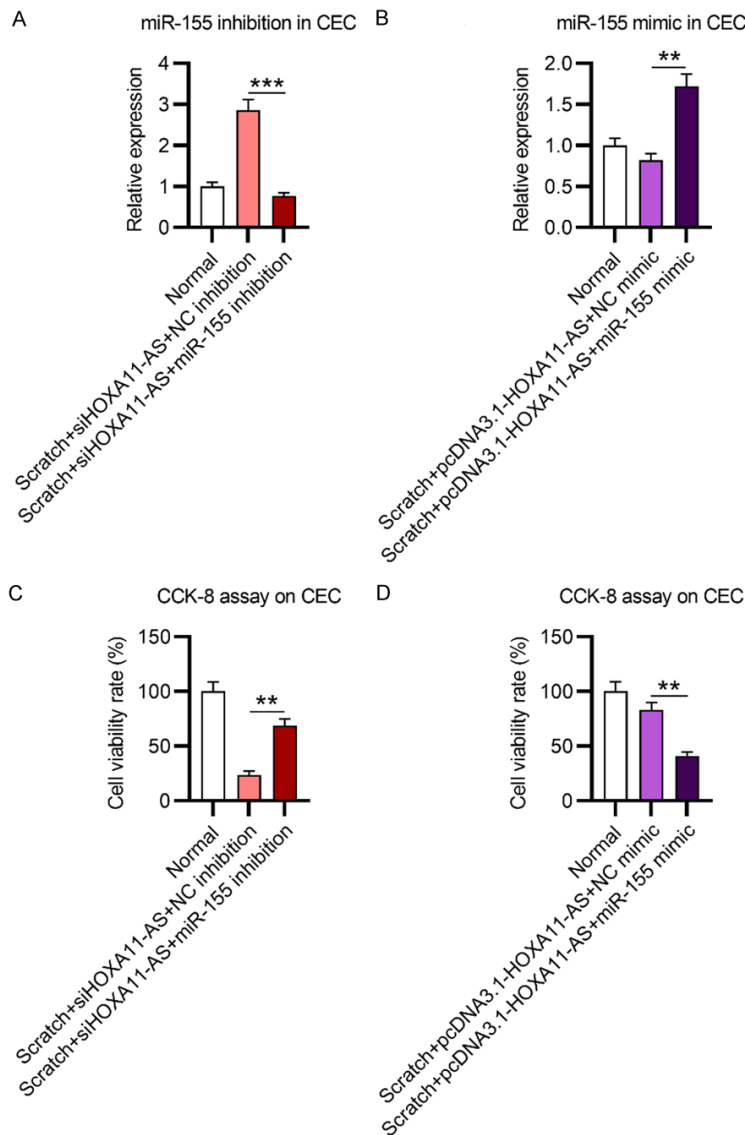


Figure 6. Role of miR-155 in the HOXA11-AS-mediated attenuation of viability in injured B4G12 cells. Wounds on B4G12 cells were made by scratching via a sterile pipette tip. B4G12 cells were transfected with siRNA-HOXA11-AS and NC/miR-155 inhibitor or pcDNA3.1-HOXA11-AS and NC/miR-155 mimic and then collected at 12 h after scratches for further analyses. A, B. HOXA11-AS expression in B4G12 cells was determined via qRT-PCR. C, D. B4G12 cell viability was examined by a CCK-8 assay. ** $P < 0.01$, *** $P < 0.001$.

contributed to a higher rate of migration in B4G12 cells with silenced HOXA11-AS than in the control group (Figure 8A). ZO-1 and N-cadherin expression levels were also elevated after miR-155 inhibition (Figure 8B). On the other hand, miR-155 mimic transfection in HOXA11-AS-overexpressing and scratch-injured CECs caused a reduction in migration and decreased ZO-1 and N-cadherin expression levels (Figure 8C, 8D). Collectively, these data suggested that miR-155 abolished the effect of

HOXA11-AS on the migration of scratch-injured B4G12 cells.

E2F2 is a downstream target of the HOXA11-AS-miR-155 axis in B4G12 cells during injury

Previous studies have demonstrated that the 3'-untranslated region (UTR) of the *E2F2* gene acts as a target of miR-155 [25, 26], and a recent report has shown that *E2F2* is responsible for the miR-155-regulated cell cycle and barrier function of CECs in myopia [27]. Here, we examined the protein level of *E2F2* in scratch-injured B4G12 cells to understand the correlation between *E2F2* expression and the HOXA11-AS-miR-155 axis. Bioinformatics-based prediction also confirmed that miR-155 might target the 3'-UTR of *E2F2* (Figure 9A). A dual luciferase assay showed that the activity of luciferase fused to the wild-type 3'-UTR of *E2F2* was reduced by half following transfection with the miR-155 mimic compared to that in the control group (Figure 9B). *E2F2* expression in injured B4G12 cells was lower than that in non-injured control cells. HOXA11-AS silencing in injured B4G12 cells caused the downregulation of *E2F2* expression, while the overexpression of HOXA11-AS led to the upregulation of

E2F2. Furthermore, miR-155 counteracted the effect of HOXA11-AS on *E2F2* expression in B4G12 cells (Figure 9C). These data suggested that *E2F2* was a downstream target of the HOXA11-AS-miR-155 axis in B4G12 cells during scratch wounding.

Discussion

In vivo, CECs are arrested in the G1 phase of the cell cycle and are actively maintained in a

HOXA11-AS in corneal endothelial injury

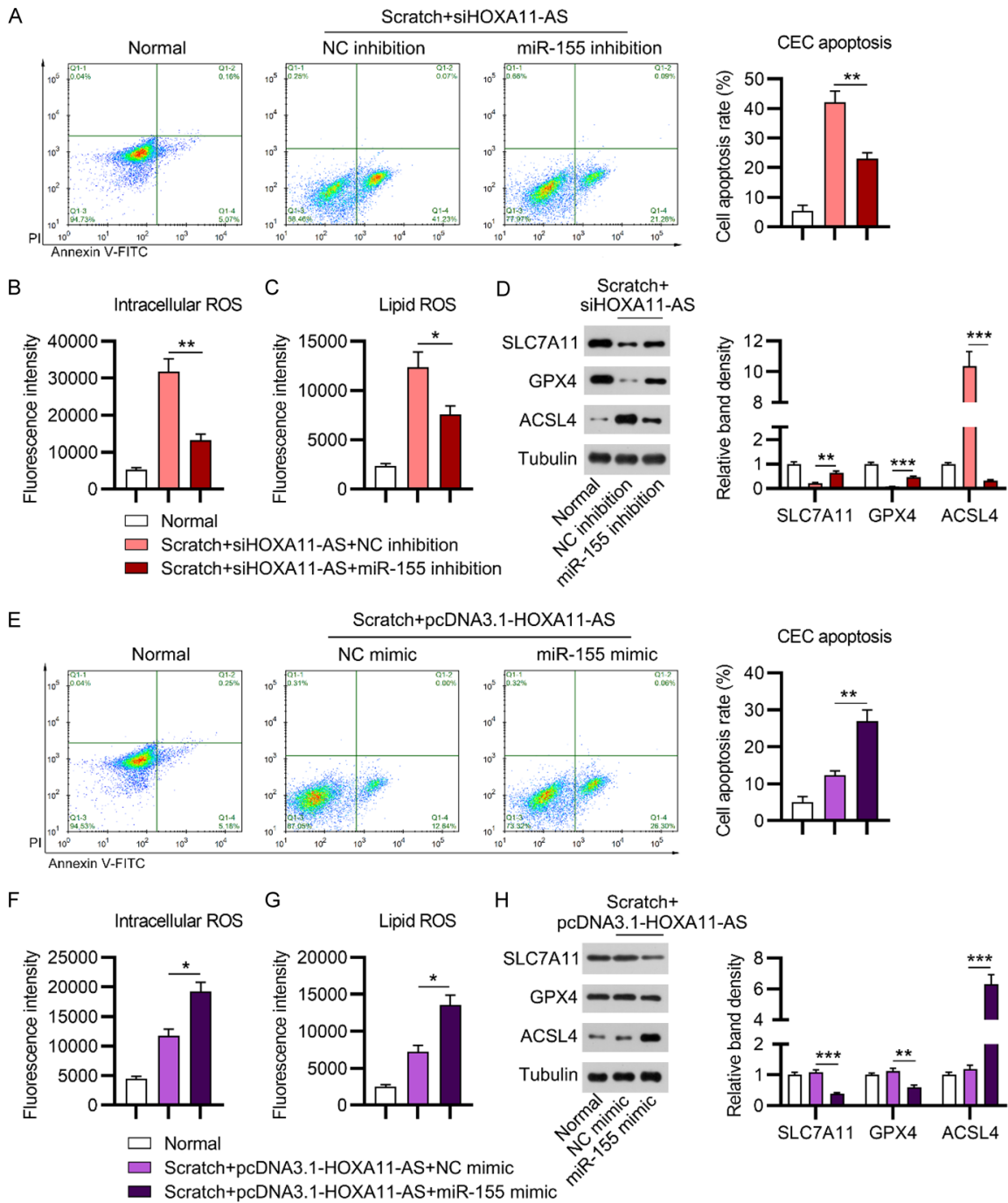


Figure 7. Contribution of miR-155 to the HOXA11-AS-mediated reduction in ferroptosis in B4G12 cells. Wounds on B4G12 cells were made by scratching via a sterile pipette tip. B4G12 cells were transfected with siRNA-HOXA11-AS and NC/miR-155 inhibitor or with pcDNA3.1-HOXA11-AS and NC/miR-155 mimic and collected at 12 h after scratches for subsequent analyses. (A, E) Apoptotic cells were counted by FC. The rate of apoptosis in each group is shown on the right-hand panel. (B, F) DCFH-DA and (C, G) C11 BODIPY staining were performed to evaluate the production of intracellular and lipid ROS in B4G12 cells, respectively. (D, H) WB results for the expression of GPX4, ACSL4, and SLC7A11 in B4G12 cells. *P < 0.05, **P < 0.01, ***P < 0.001.

non-proliferative state. After injury, cells with endothelial phenotypes acquire the capacity for proliferation; however, this is insufficient to resolve large wounds. Corneal surgery, external

trauma, and stress from endothelial dystrophies or glaucoma may dramatically decrease the endothelial cell density, causing residual CEC decompensation [28]. In addition, the bar-

HOXA11-AS in corneal endothelial injury

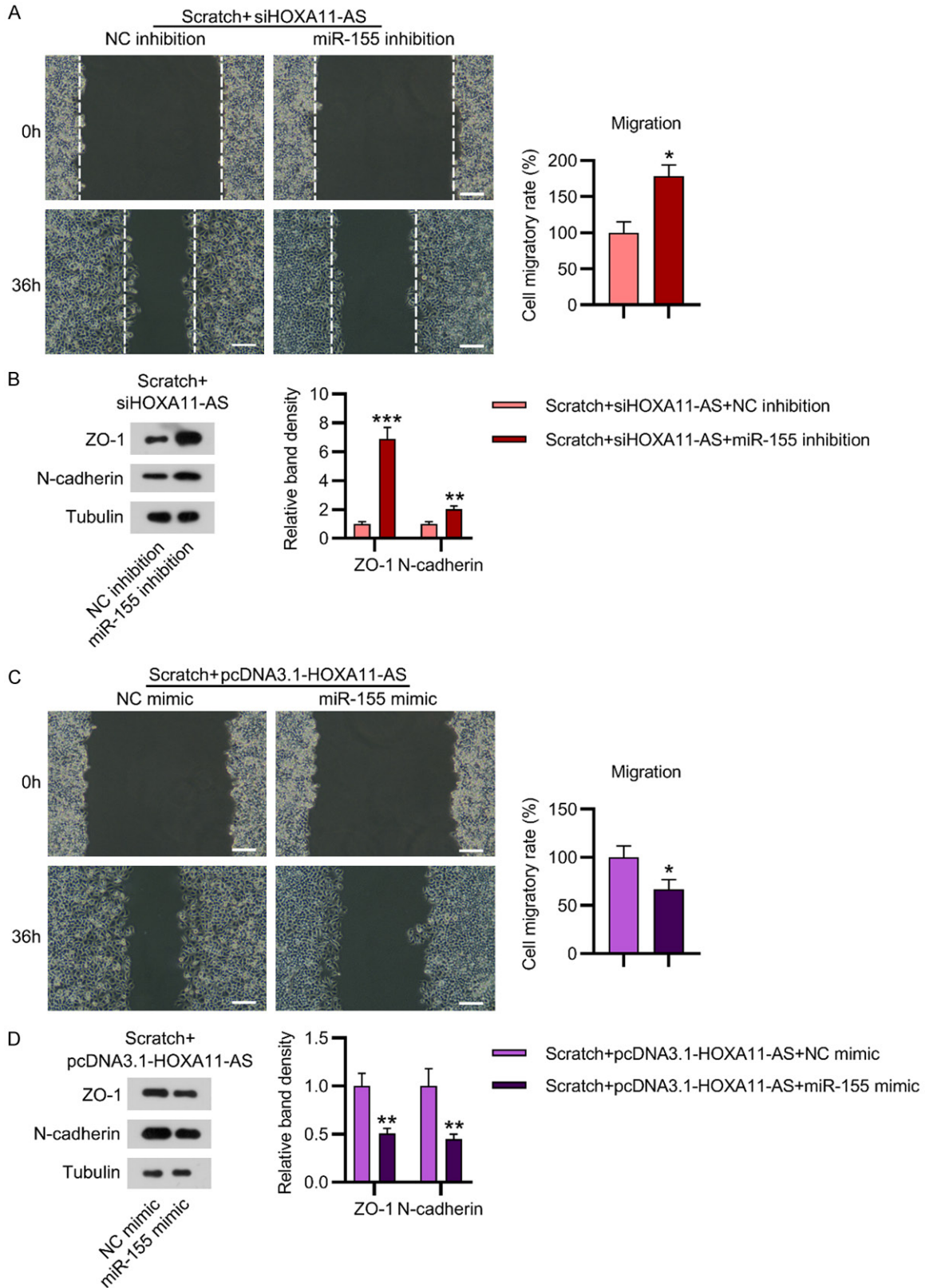


Figure 8. Involvement of miR-155 in the HOXA11-AS-mediated migration of scratch-injured B4G12 cells. B4G12 cells were scratched via a sterile pipette tip. B4G12 cells were transfected with siRNA-HOXA11-AS and NC/miR-155 inhibitor or co-transfected with pcDNA3.1-HOXA11-AS and NC/miR-155 mimic and then collected at 12 h after scratches for further analysis. A, C. Cell migration rate of B4G12 cells was determined using a scratch wound assay. B, D. ZO-1 and N-cadherin protein expression levels were examined by WB.

HOXA11-AS in corneal endothelial injury

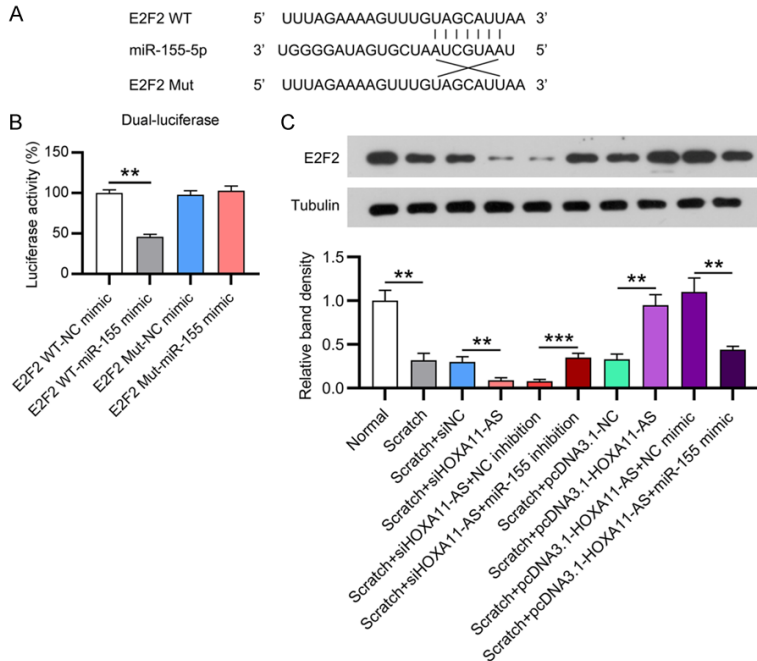


Figure 9. E2F2 is a miR-155 target gene. A. Graphical representation of the conserved 3'-UTR E2F2 binding motif of miR-155. B. Dual-luciferase reporter assay (DLRA) using luciferase reporter constructs containing either mutant (Mut) or wild-type (WT) 3'-UTR E2F2 transfected with the miR-155/NC mimic. Firefly luciferase activity was normalized to Renilla luciferase activity, which was used as the reference. C. B4G12 cells were transfected with siRNA-HOXA11-AS, pcDNA3.1-HOXA11-AS, or corresponding negative controls, co-transfected with siRNA-HOXA11-AS and NC/miR-155 inhibitor or pcDNA3.1-HOXA11-AS and NC/miR-155 mimics, and collected 12 h after scratch wounding for further analysis. WB was used to detect the protein level of E2F2 in B4G12 cells. * $P < 0.05$, ** $P < 0.01$, *** $P < 0.001$.

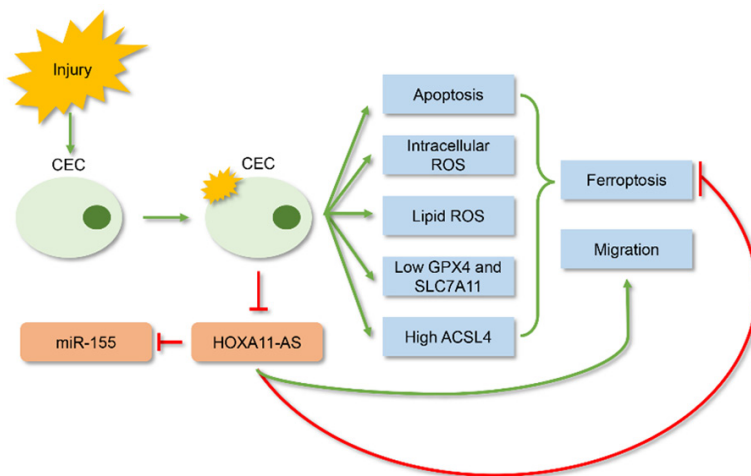


Figure 10. Schematic diagram of the effects of HOXA11-AS during CEC damage. Scratch-injured B4G12 cells showed high levels of ferroptosis and migration. HOXA11-AS expression was downregulated, while miR-155 expression was upregulated, in scratch-injured B4G12 cells. HOXA11-AS overexpression decreased ferroptosis, as evidenced by decreases in apoptosis, intracellular and lipid ROS production, and ferroptotic protein expression. HOXA11-AS promoted the migration of injured B4G12 cells.

rier function, including ZO-1 and N-cadherin functions, and migration of cells are important for maintaining visual acuity; however, any abnormality in barrier-related proteins may damage their function [29, 30]. Based on the post-transcriptional modulatory function of lncRNAs, we hypothesized that the lncRNA HOXA11-AS is involved in the proliferation, barrier function, and migration of CECs during scratch wounding. In the present study, HOXA11-AS expression was lower, while miR-155 expression was higher, in the corneal endothelium of CEI-treated mice and scratch-injured B4G12 cells than in control cells, suggesting that dysregulated HOXA11-AS and miR-155 are related to CEI. Additional bioinformatic analyses and dual-luciferase reporter assay results suggest that there is an inverse correlation between HOXA11-AS and miR-155 (Figure 10).

Recently, the ferroptotic mode of programmed necrosis has been identified as a form of cell death independent of apoptosis [31]. Ferroptosis is mostly promoted by lipid peroxidation and is modulated at many levels, including by iron metabolism and antioxidant pathways [32]. Ferroptosis is characterized by iron-dependent, robust lipid ROS accumulation [33-35]. Enzymes used to modify chromatin mediate the sensing of intermediary metabolic products to regulate gene modulation and disease (e.g., cancer) development [36-38]. To the best of our knowledge, this study is the first to demonstrate that ferroptosis participates in CEI development, and the overexpression of HOXA11-AS exerts

an inhibitory effect on ferroptosis by mediating miR-155 expression in CECs, providing a novel mechanism underlying CEI.

HOXA11-AS is an HOX A11 antisense lncRNA. In the human genome, the HOX gene family features highly conserved homeodomains [39]. HOXA11-AS may be involved in embryonic implantation, cervical carcinogenesis, and endometrial progression by modulating HOXA11 expression [40]. There is accumulating evidence that HOXA11-AS could serve as a new modulator of the metastasis and proliferation of various human cancers [22, 41, 42]. However, the role of HOXA11-AS in other diseases, including CEI, has rarely been reported. Our findings clearly demonstrate that HOXA11-AS expression level is reduced in the injured corneal endothelium and scratch-injured CECs. The silencing of HOXA11-AS aggravated cell damage, as evidenced by impaired cell viability and elevated ferroptosis. HOXA11-AS overexpression partially restored the cell survival rate after scratch wounding. Moreover, HOXA11-AS promoted the barrier function and rate of migration of CECs, suggesting that HOXA11-AS has a protective function against CEI.

In summary, our findings demonstrated that the lncRNA HOXA11-AS in CECs promotes survival, inhibits ferroptosis, and improves barrier function and migration during injury by sponging miR-155. However, the results were not confirmed in an animal model of CEI, which will be addressed in our future work. Our findings demonstrated that the HOXA11-AS/miR-155 axis may be a therapeutic target for CEI.

Disclosure of conflict of interest

None.

Address correspondence to: Xiaoyong Yuan, Tianjin Key Laboratory of Ophthalmology and Visual Science, Tianjin Eye Institute, Tianjin Eye Hospital, No. 4 Gansu Road, He-ping District, Tianjin 300000, China. Tel: +86-15222061900; E-mail: yuan_xy1234@126.com

References

[1] Petroll WM, Hsu JK, Bean J, Cavanagh HD and Jester JV. The spatial organization of apical junctional complex-associated proteins in feline and human corneal endothelium. *Curr Eye Res* 1999; 18: 10-19.

- [2] Bonanno JA. Molecular mechanisms underlying the corneal endothelial pump. *Exp Eye Res* 2012; 95: 2-7.
- [3] Zhang W, Frausto R, Chung DD, Griffis CG, Kao L, Chen A, Azimov R, Sampath AP, Kurtz I and Aldave AJ. Energy shortage in human and mouse models of SLC4A11-Associated corneal endothelial dystrophies. *Invest Ophthalmol Vis Sci* 2020; 61: 39.
- [4] Ong HS, Peh G, Neo DJH, Ang HP, Adnan K, Nyein CL, Morales-Wong F, Bhogal M, Kocaba V and Mehta JS. A novel approach of harvesting viable single cells from donor corneal endothelium for cell-injection therapy. *Cells* 2020; 9: 1428.
- [5] Hwang JS, Yi HC and Shin YJ. Effect of SOX2 repression on corneal endothelial cells. *Int J Mol Sci* 2020; 21: 4397.
- [6] Okumura N and Koizumi N. Regeneration of the corneal endothelium. *Curr Eye Res* 2020; 45: 303-312.
- [7] Bu J, Yu J, Wu Y, Cai X, Li K, Tang L, Jiang N, Jeyalatha MV, Zhang M, Sun H, He H, Quantock AJ, Chen Y, Liu Z and Li W. Hyperlipidemia affects tight junctions and pump function in the corneal endothelium. *Am J Pathol* 2020; 190: 563-576.
- [8] Sie NM, Yam GH, Soh YQ, Lovatt M, Dhaliwal D, Kocaba V and Mehta JS. Regenerative capacity of the corneal transition zone for endothelial cell therapy. *Stem Cell Res Ther* 2020; 11: 523.
- [9] Morishige N and Sonoda KH. Bullous keratopathy as a progressive disease: evidence from clinical and laboratory imaging studies. *Cornea* 2013; 32 Suppl 1: S77-83.
- [10] Okumura N, Inoue R, Okazaki Y, Nakano S, Nakagawa H, Kinoshita S and Koizumi N. Effect of the rho kinase inhibitor Y-27632 on corneal endothelial wound healing. *Invest Ophthalmol Vis Sci* 2015; 56: 6067-6074.
- [11] Okumura N, Okazaki Y, Inoue R, Kakutani K, Nakano S, Kinoshita S and Koizumi N. Effect of the rho-associated kinase inhibitor eye drop (ripasudil) on corneal endothelial wound healing. *Invest Ophthalmol Vis Sci* 2016; 57: 1284-1292.
- [12] Kinoshita S, Koizumi N, Ueno M, Okumura N, Imai K, Tanaka H, Yamamoto Y, Nakamura T, Inatomi T, Bush J, Toda M, Hagiya M, Yokota I, Teramukai S, Sotozono C and Hamuro J. Injection of cultured cells with a rock inhibitor for bullous keratopathy. *N Engl J Med* 2018; 378: 995-1003.
- [13] Zhang W, Chen J, Fu Y and Fan X. The signaling pathway involved in the proliferation of corneal endothelial cells. *J Recept Signal Transduct Res* 2015; 35: 585-591.

HOXA11-AS in corneal endothelial injury

- [14] Parekh M, Ferrari S, Sheridan C, Kaye S and Ahmad S. Concise review: an update on the culture of human corneal endothelial cells for transplantation. *Stem Cells Transl Med* 2016; 5: 258-264.
- [15] Chan JJ and Tay Y. Noncoding RNA:RNA regulatory networks in cancer. *Int J Mol Sci* 2018; 19: 1310.
- [16] Schmitt AM and Chang HY. Long noncoding RNAs: at the intersection of cancer and chromatin biology. *Cold Spring Harb Perspect Med* 2017; 7: a026492.
- [17] Bolha L, Ravnik-Glavač M and Glavač D. Long noncoding RNAs as biomarkers in cancer. *Dis Markers* 2017; 2017: 7243968.
- [18] Guttman M and Rinn JL. Modular regulatory principles of large non-coding RNAs. *Nature* 2012; 482: 339-346.
- [19] Dhamija S and Diederichs S. From junk to master regulators of invasion: lncRNA functions in migration, EMT and metastasis. *Int J Cancer* 2016; 139: 269-280.
- [20] Xu J, Bo Q, Zhang X, Lei D, Wang J and Pan X. lncRNA HOXA11-AS promotes proliferation and migration via sponging miR-155 in hypopharyngeal squamous cell carcinoma. *Oncol Res* 2020; 28: 311-319.
- [21] Sun M, Nie F, Wang Y, Zhang Z, Hou J, He D, Xie M, Xu L, De W, Wang Z and Wang J. lncRNA HOXA11-AS promotes proliferation and invasion of gastric cancer by scaffolding the chromatin modification factors PRC2, LSD1, and DNMT1. *Cancer Res* 2016; 76: 6299-6310.
- [22] Chen JH, Zhou LY, Xu S, Zheng YL, Wan YF and Hu CP. Overexpression of lncRNA HOXA11-AS promotes cell epithelial-mesenchymal transition by repressing miR-200b in non-small cell lung cancer. *Cancer Cell Int* 2017; 17: 64.
- [23] Nakano Y, Oyamada M, Dai P, Nakagami T, Kinoshita S and Takamatsu T. Connexin43 knockdown accelerates wound healing but inhibits mesenchymal transition after corneal endothelial injury in vivo. *Invest Ophthalmol Vis Sci* 2008; 49: 93-104.
- [24] Livak KJ and Schmittgen TD. Analysis of relative gene expression data using real-time quantitative PCR and the $2^{-\Delta\Delta C(T)}$ method. *Methods* 2001; 25: 402-408.
- [25] Li T, Yang J, Lv X, Liu K, Gao C, Xing Y and Xi T. MiR-155 regulates the proliferation and cell cycle of colorectal carcinoma cells by targeting E2F2. *Biotechnol Lett* 2014; 36: 1743-1752.
- [26] Gao Y, Ma X, Yao Y, Li H, Fan Y, Zhang Y, Zhao C, Wang L, Ma M, Lei Z and Zhang X. miR-155 regulates the proliferation and invasion of clear cell renal cell carcinoma cells by targeting E2F2. *Oncotarget* 2016; 7: 20324-20337.
- [27] Yuan S, He G and Li L. Hsa-miR-155 regulates the cell cycle and barrier function of corneal endothelial cells through E2F2. *Am J Transl Res* 2021; 13: 1505-1515.
- [28] Joyce NC. Proliferative capacity of the corneal endothelium. *Prog Retin Eye Res* 2003; 22: 359-389.
- [29] Wang F, Wang D, Song M, Zhou Q, Liao R and Wang Y. MiRNA-155-5p reduces corneal epithelial permeability by remodeling epithelial tight junctions during corneal wound healing. *Curr Eye Res* 2020; 45: 904-913.
- [30] Hara S, Tsujikawa M, Maruyama K and Nishida K. STAT3 signaling maintains homeostasis through a barrier function and cell survival in corneal endothelial cells. *Exp Eye Res* 2019; 179: 132-141.
- [31] Shaw AT, Winslow MM, Magendantz M, Ouyang C, Dowdle J, Subramanian A, Lewis TA, Maglathin RL, Tolliday N and Jacks T. Selective killing of K-ras mutant cancer cells by small molecule inducers of oxidative stress. *Proc Natl Acad Sci U S A* 2011; 108: 8773-8778.
- [32] Wu S, Zhu C, Tang D, Dou QP, Shen J and Chen X. The role of ferroptosis in lung cancer. *Biomark Res* 2021; 9: 82.
- [33] Yang WS, SriRamaratnam R, Welsch ME, Shimada K, Skouta R, Viswanathan VS, Cheah JH, Clemons PA, Shamji AF, Clish CB, Brown LM, Girotti AW, Cornish VW, Schreiber SL and Stockwell BR. Regulation of ferroptotic cancer cell death by GPX4. *Cell* 2014; 156: 317-331.
- [34] Dixon SJ and Stockwell BR. The role of iron and reactive oxygen species in cell death. *Nat Chem Biol* 2014; 10: 9-17.
- [35] Jiang Y, Mao C, Yang R, Yan B, Shi Y, Liu X, Lai W, Liu Y, Wang X, Xiao D, Zhou H, Cheng Y, Yu F, Cao Y, Liu S, Yan Q and Tao Y. EGLN1/c-Myc induced lymphoid-specific helicase inhibits ferroptosis through lipid metabolic gene expression changes. *Theranostics* 2017; 7: 3293-3305.
- [36] He Y, Gao M, Cao Y, Tang H, Liu S and Tao Y. Nuclear localization of metabolic enzymes in immunity and metastasis. *Biochim Biophys Acta Rev Cancer* 2017; 1868: 359-371.
- [37] He X, Yan B, Liu S, Jia J, Lai W, Xin X, Tang CE, Luo D, Tan T, Jiang Y, Shi Y, Liu Y, Xiao D, Chen L, Liu S, Mao C, Yin G, Cheng Y, Fan J, Cao Y, Muegge K and Tao Y. Chromatin remodeling factor LSH drives cancer progression by suppressing the activity of fumarate hydratase. *Cancer Res* 2016; 76: 5743-5755.
- [38] Liu S and Tao Y. Interplay between chromatin modifications and paused RNA polymerase II in dynamic transition between stalled and activated genes. *Biol Rev Camb Philos Soc* 2013; 88: 40-48.
- [39] Xue JY, Huang C, Wang W, Li HB, Sun M and Xie M. HOXA11-AS: a novel regulator in human cancer proliferation and metastasis. *Onco Targets Ther* 2018; 11: 4387-4393.

HOXA11-AS in corneal endothelial injury

- [40] Chen J, Fu Z, Ji C, Gu P, Xu P, Yu N, Kan Y, Wu X, Shen R and Shen Y. Systematic gene microarray analysis of the lncRNA expression profiles in human uterine cervix carcinoma. *Biomed Pharmacother* 2015; 72: 83-90.
- [41] Liu Z, Chen Z, Fan R, Jiang B, Chen X, Chen Q, Nie F, Lu K and Sun M. Over-expressed long noncoding RNA HOXA11-AS promotes cell cycle progression and metastasis in gastric cancer. *Mol Cancer* 2017; 16: 82.
- [42] Li W, Jia G, Qu Y, Du Q, Liu B and Liu B. Long Non-Coding RNA (LncRNA) HOXA11-AS promotes breast cancer invasion and metastasis by regulating epithelial-mesenchymal transition. *Med Sci Monit* 2017; 23: 3393-3403.